HHS Public Access

Author manuscript

*Physiol Behav*. Author manuscript; available in PMC 2016 December 01.

Published in final edited form as:

*Physiol Behav*. 2015 December 1; 152(0 0): 329–339. doi:10.1016/j.physbeh.2015.07.025.

# Effects of High-Fat Diet and Gastric Bypass on Neurons in the Caudal Solitary Nucleus

**AJ Boxwell**[1], **Z Chen**[1], **CM Mathes**[2], **AC Spector**[2], **CW Le Roux**[3], **SP Travers**[1], and **JB Travers**[1]

[1]Ohio State Univ., Columbus, OH, United States [2]Florida State Univ., Tallahassee, FL, United States [3]Univ. College Dublin, Dublin, Ireland

## 1. Introduction

Roux-en-Y gastric bypass surgery (RYGB) is an effective procedure for reversing morbid obesity (Attiah, Halpern et al. 2012; Leslie, Dorman et al. 2012; Mingrone, Panunzi et al. 2012). The explanations for its efficacy likely include complex interactions between the peripheral and central nervous system (Berthoud, Shin et al. 2011; Lutz and Bueter 2014). Proposed mechanisms for weight loss include increased energy expenditure, enhanced satiety signals, and changes in the preference for certain foods. The caudal nucleus of the solitary tract (cNST) may well play a role in these proposed mechanisms. It receives neural and hormonal satiety signals from the gut (Dockray 2009; de Lartigue, de La Serre et al. 2011), projects to brainstem structures involved in regulating metabolism, e.g. (Zechner, Mirshahi et al. 2013; Lutz and Bueter 2014), and has reciprocal connections with forebrain structures involved in food regulation and preference (Rinaman 2010; Rinaman 2011). Moreover, it shows demonstrable plasticity in response to short-term changes in energy balance (Rinaman, Baker et al. 1998) as well as changes associated with diet (Covasa, Grahn et al. 2000).

Although several studies have demonstrated altered sensitivity of vagal sensory neurons and their central connections in response to a high fat diet (HFD), fewer studies have examined the effects of RYGB on these neurons. As initially demonstrated by the Ritter lab (Covasa, Grahn et al. 2000), rats maintained on a high fat diet showed less fos-like immunoreactivity (FLI) in the cNST in response to the satiety peptide cholecystokinin (CCK), compared to rats on a normal diet. Some of this change in cNST responsiveness appears to reflect altered peripheral input. Thus, more recently, the HFD-induced reduction in cNST FLI in response to CCK or a macronutrient load was correlated with a reduction in CCK-1 receptor expression in the mouse nodose ganglion (Nefti, Chaumontet et al. 2009). Several other

Address correspondence to: Joseph Travers, PhD, The Ohio State University, 305 w 12th ave, Columbus, OH 43210, (614) 292 6365 (office), 614 247 6945 (FAX), Travers.1@osu.edu.

studies have demonstrated reduced sensitivity of vagal afferents in animals fed a high fat diet, including decreased responsiveness of jejunal afferents to CCK and stretch, accompanied by a decrease in neuronal excitability, including a higher threshold and lowered membrane resistance (Daly, Park et al. 2011). In another study, a HFD was associated with reduced responsiveness of gastric vagal tension receptors, accompanied by a decrease in receptor expression for the orexogenic gastric peptide, ghrelin (Kentish, Li et al. 2012).

Vagal efferent neurons in the dorsal motor nucleus (DMN) also showed reduced excitability following a HFD (Browning, Fortna et al. 2013). This was evident based on a lowered membrane resistance, an increase in the transient outward current (TOC) $I_A$, and a suppressed response to the satiety peptides, CCK and glucagon-like peptide 1 (GLP-1). Moreover, these effects were reduced by RYGB (Browning, Fortna et al. 2013). There is little work, however on the effects of RYGB on cNST neurons. One study showed that RYGB increased levels of feeding-induced FLI in the cNST, perhaps reflecting an enhanced satiety signal (Berthoud, Shin et al. 2011). The present study used an *in vitro* preparation to determine the impact of a HFD and RYGB on the cellular properties and solitary tract driven responses of cNST neurons. Similar recordings were made from slices of the rostral (orosensory) nucleus of the solitary tract (rNST) since there is some evidence for taste preference changes following RYGB surgery (Hajnal, Kovacs et al. 2010; Berthoud, Shin et al. 2011; Tichansky, Glatt et al. 2011; Mathes and Spector 2012; Lutz and Bueter 2014).

## 2. Materials and Methods

### 2.1. Animals

Twenty-six male Sprague-Dawley rats were used in this study. Four experimental groups consisted of 15 sham operated animals, 7 on a normal chow diet and 8 on a HFD (Research Diets D12492: 60% calories from fat), and 11 RYGB animals, 3 on normal chow (CHOW) and 8 on a HFD. Animals were shipped from Florida State University where they had been used in a series of behavioral studies over a period of several months (Mathes, Bohnenkamp et al. 2015). Prior to these behavioral tests, all animals were injected with an ivermectin suspension 1/wk for 10 weeks for pinworms (Ivomec, Merial; 1% diluted in propylene glycol: 600 μg/Kg,sc). The behavioral studies included the use of mild water or food deprivation and the injection of Octreotide (IP: 30μg/kg) in all animals. Approximately 4 weeks transpired between the Octreotide infusion and their use in the present study (see Fig. 1 timeline). Animals were maintained on the diets described above throughout the studies at Florida State and Ohio State University. All procedures were approved by the Animal Care and Use Committee at both Florida State University and the Ohio State University.

### 2.2. Surgical Procedure

Rats underwent either RYGB surgery or a sham operation prior to behavioral testing and the surgical procedures are described in that report (Mathes, Bohnenkamp et al. 2015), and elsewhere (e.g., (Bueter, Abegg et al. 2012; Mathes, Bueter et al. 2012). Briefly, the RYGB operation entails 1) the construction of an anastomosis between a small portion of the stomach continuous with the esophagus (~4–5 mm) and the proximal jejunum (15 cm aboral

of the pylorus), creating the alimentary limb through which ingested food descends; 2) the construction of an anastomosis of the proximal jejunum (15 cm aboral of the pylorus) continuous with the remaining majority of the stomach with the distal jejunum (25 cm oral of the cecum), creating the bileopancreatic limb through which digestive juices are transported; and 3) the remaining distal jejunum and ileum, which is referred to as the common channel and is the site where food and digestive juices mix. The SHAM operation consists of sutures placed at the sites of intestinal reorganization in the RYGB. Both surgeries were conducted using aseptic technique while the rats were under isoflurane anesthesia (2–5% delivered in oxygen at 1 l/min). An analgesic (carprofen [Rimadyl]; 5 mg/kg) and an antibiotic (enrofloxycin [Baytril]; 2.3 mg/kg) were injected sc immediately preceding and daily for 3 days following surgery.

### 2.3. Slice Preparation

Following arrival at Ohio State University, animals were adapted to their new location for 2 weeks and weighed daily to ensure no untoward effects of transport. To make certain that all animals were subject to the same metabolic condition at the time of recording, rats were fasted overnight and then given 3 g of chow 1 hour before sacrifice. Acute slices were prepared for electrophysiological recording following anesthetization with isoflurane, decapitation, and rapid removal and cooling of the brain. The blocked brainstem was glued to a ceramic block using cyanoacrylate glue, and coronal brainstem slices 250 μm thick were cut with a sapphire blade on a vibratome (model 1000, Vibratome, St. Lois, MO, USA) in an ice-cold carboxygenated cutting solution containing (in mM) 110 choline, 25 $NaHCO_3$, 3 KCl, 7 $MgSO_4$, 1.5 $NaH_2PO_4$, 10 d-Glucose, 0.5 $CaCl_2$. Slices were divided into two series (rNST and cNST) to allow simultaneous recording by two investigators, both blind to the diet/surgical condition of the rat. Slices were incubated in a carboxgyenated artificial cerebrospinal fluid (ACSF) containing (in mM) 124 NaCl, 25 $NaHCO_3$, 3 KCl, 1 $MgSO_4$, 1.5 $NaH_2PO_4$, 10 d-Glucose, and 1.5 $CaCl_2$ at 32°C for one hour prior to recording.

Slices were transferred to a recording chamber and perfused with 36°C ACSF at a rate of 1–2 mL/minute. Neurons identified using DIC optics were recorded in whole cell patch clamp using a 4–6 MΩ pulled glass pipettes filled with an intracellular solution containing (in mM) 130 K-gluconate, 10 EGTA, 10 HEPES, 1 $CaCl_2$, 1 $MgCl_2$, and 2 ATP, at pH 7.2–7.3 and osmolality 290–295 mOsm. Lucifer yellow (0.05%) was added to the intracellular solution. An initial seal of greater than 1 GΩ and a membrane resistance of greater than 100 mΩ were inclusion criteria for seal and cell viability. Recordings were made with an A-M Systems Model 2400 amplifier (rNST) or an Axon Instruments Axopatch 200B amplifier (cNST), using pClamp software (Molecular Devices, Sunnyvale, CA).

### 2.4. Recording Protocols

**2.4.1. Response to afferent stimulation—**The NST and solitary tract (ST) were visualized with a Nikon E600FN microscope and a bipolar stimulating electrode made of twisted insulated wire was placed on the ST under visual control. Stimulation of the ST consisted of two current pulses 0.15 ms in duration delivered at 0.3 hertz. For each neuron, we constructed recruitment plots by graphing the mean EPSC amplitude ± SEM (from 3–6 replications) at 18 intensity levels (1 – 150 μA). We did not exceed 150 uA for ST

stimulation because we were concerned about current spread in the tissue that might result in direct activation of NST interneurons rather than ST fibers. The threshold to elicit a postsynaptic response was defined as the stimulation current that evoked a response in which the error bars did not overlap with the next lowest level of stimulation.

**2.4.2. Membrane Properties—**Under current clamp, 250 ms current pulses ranging from −0.1 nA to 0.6 nA in 0.02 nA increments were applied. As an index of neuron excitability, membrane voltage was measured for each level below threshold and the number of evoked action potentials counted at each level above threshold. Peak action potential amplitude, half-width and the amplitude of the after-hyperpolarization were calculated from the threshold for the action potential defined as the inflection point on the rising phase using standard templates in Clampfit (Suwabe, Mistretta et al. 2011). In a second protocol under voltage clamp, we assessed the presence and magnitude of an "$I_A$-like" transient outward current (TOC). After a 1 second holding period at −100 mV, we stepped the membrane potential to voltages between −100 and −40 mV (5 mV step size) for 2 seconds and measured the peak TOCs (activation curve). We followed this step with a 2 second step to −40 mV and measured the peak TOCs resulting from this second step (inactivation curve). The peak TOCs were calculated as the difference between the peak outward current and the sustained current at the end of the 2 sec activation protocol, when the membrane current had stabilized. Membrane resistance was calculated using the sustained current values between −80 and −70 mV. The data were not corrected for liquid junction potentials. In order to analyze driven afferent input and action potential characteristics, we did not use TTX or other channel blockers in the bath. In order to avoid contamination by voltage gated sodium channels, we did not extend our holding potential above −40 mV.

**2.4.3. Response to Drugs—**To determine if diet or RYGB surgery affected cNST neuron responses to the satiety-related peptide GLP-1, the GLP-1 analog, Exendin-4 (100nM) (Bachem, Torrance, CA) was applied to the bath solution during afferent stimulation at 150 μA (Gaisano, Park et al. 2009). Following a baseline period, the drug was applied followed by the GLP-1 antagonist, Extendin-9 (6 min each). The ST was stimulated every 18 sec (150 μA; 0.15 ms duration) over the course of each period. Testing terminated with washout. Only 1 neuron per slice was tested for drug effects, and no additional neurons in that slice were tested following drug treatment. Neurons in the rNST were similarly tested with 20 μM norepinephrine (NE) (Sigma Aldrich, MO). We chose to test NE because previous data in our lab has shown that NE modulates rNST responses and also because the rNST receives input from A2 cNST neurons (Chen, Breza et al. 2013), a population of cells that are sensitive to satiety-inducing procedures (Rinaman 2011). For the driven responses, an ANOVA compared the response amplitudes for 20 stimulations before, during and after drug application. The amplitudes and frequencies of spontaneous EPSCs (sEPSCs) were similarly quantified using Synaptosoft software. Frequency and amplitude distributions were compared using a Kolmogorov-Smirov test with a significance criteria set at $P < .05$.

## 2.5. Post-hoc histology

Following the recording experiments, slices were fixed in paraformaldehyde and processed using standard immunohistochemical techniques for the ionotropic purinergic receptor,

P2X2 (P2X2r) and for dopamine-beta-hydroxylase (DBH) (Banihashemi and Rinaman 2006; Bartel 2012). P2X2r immunostaining is an excellent method for visualizing the borders and key structures of the NST because it selectively labels the solitary tract and a subset of the primary afferent terminal field (Ganchrow, Ganchrow et al. 2014); in particular in the rNST the terminal field is believed to arise from gustatory-responsive neurons (Bartel 2012). We were further interested in determining if recorded neurons in the cNST belonged to the A2 group. Photomicrographs were taken of labeled neurons and compared to photomicrographs taken during recording. Cell locations in the cNST were categorized according to their locations relative to the area postrema and solitary tract. In the rostral NST, cell locations were similarly categorized by their relative locations between the point at which the NST moves lateral to the IVth ventricle and the rostral pole of the nucleus and assigned a location according to a standard atlas of the rat brain (Paxinos and Watson 1986). When post-hoc P2X2r fiber staining was robust, we also noted whether recorded neurons were within the P2X2r field.

### 2.6. Data Analysis

Data were analyzed with ANOVA or chi-square as appropriate, using SYSTAT (version 13). The critical value for significance was set at $P < .05$.

## 3. Results

### 3.1. Animals

Animals on the HFD weighed significantly more than those on normal chow, and those subjected to the RYGB weighed less than sham-operated controls (ANOVA, diet, $P < .009$; surgery, $P < .001$, interaction, n.s., Fig. 2, Table 1). Hematocrit levels were significantly lower following RYGB ($P < .005$) but not enough to be classified as anemic (Bogdanske, Hubbard-Van Stelle et al. 2011). Diet had no effect on the hematocrit level. Based on trunk blood collected at the time of decapitation (60 min post-meal), glucose levels were not significantly different across the 4 groups ($P > .05$).

### 3.2. Caudal solitary nucleus

**3.2.1. Cell location—**Cell locations were classified into 1 of 3 rostral caudal levels: (1) rostral to the area postrema, (2) at the level of the area postrema, (3) caudal to the area postrema. Table 1 indicates the numbers and proportions of neurons from the 4 experimental groups at each of the 3 levels; most neurons were recorded at the level of the area postrema, e.g. (Fig. 3) and there was no difference in the proportion of cells recorded at each of the 3 levels as a function of group ($\chi^2$, $P > .05$). Although only a small number of the neurons (15/287) were stained for DBH, this probably represents an underestimate due to the suboptimal conditions for immunohistochemistry and photomicroscopy afforded by thick sections that were not fixed immediately after sacrifice. Indeed, many of the recorded cells were intermingled with the A2 population (Fig. 3C).

**3.2.2. Response to afferent stimulation—**Of 287 neurons tested, 222 (77%) had excitatory responses to solitary tract (ST) stimulation. Of these, 204 responded with excitatory postsynaptic currents (EPSCs) from which we calculated the minimum current

necessary to elicit a threshold response. There was no difference in the ST-stimulation threshold necessary for eliciting an EPSC for either diet or surgical condition (ANOVA, P > .05, Fig 4A), nor any interaction between these variables. Neither did the amplitude of the evoked EPSC at threshold vary by diet or surgical condition (Fig. 4B; ANOVA; P > .05). In contrast, there were significant effects of diet on suprathreshold responses, which were elevated with the HFD (Fig. 4D). A 3-way ANOVA across the range of stimulating currents revealed significant main effects for diet (P < .04) and current amplitude (P < .001), and an interaction between these variables (P < .001), but no main effect nor any interactions with the surgical manipulation (P's > .1). The higher amplitude suprathreshold EPSCs associated with the HFD did not seem to be a function of the number of excitatory inputs. To estimate the number of excitatory inputs, we constructed recruitment plots for each neuron by graphing the mean EPSC amplitude ± SEM (from 3–6 replications) at 18 intensity levels (1 – 150 μA). Although our protocol did not allow enough replications to measure jitter precisely enough to differentiate mono- from polysynaptic responses (Doyle and Andresen 2001), we could estimate the number of inputs by analyzing step-like breaks in the recruitment function (Fig. 4C) (Peters, Gallaher et al. 2013) (see also: (McDougall, Peters et al. 2009; Peters, McDougall et al. 2011), or in some neurons, a response at a consistently different latency. In some instances, stimulating at higher intensities produced a response decrement, suggesting recruitment of inhibitory circuits but these inhibitory inputs were not quantified. Regardless of diet or surgical condition, most neurons had from 1 – 3 inputs (P > .05, Table 2).

To gain further insight into a possible pre- versus post-synaptic source for the increase in the ST-evoked suprathreshold EPSC in the HFD group, we compared the mean frequency and amplitude of sEPSCs in a subset of neurons (N=64). There were no significant differences in amplitude or frequency as a function of diet or surgery (P's > .1).

**3.2.3. Effects of Exendin—**Bath application of Exendin-4 had only a minimal effect on either the ST-evoked response in cNST neurons or on spontaneous EPSCs. Only 6/58 neurons in which ST stimulation evoked responses showed statistically significant changes following bath application (2 decreased, 4 increased). Likewise, an analysis of the frequency of sEPSCs indicated that across 50 neurons, 7 showed increases and 7 showed decreases. Thus, there were not enough responses to perform statistics for the effects of diet and surgery.

**3.2.4. Membrane Properties—**Diet and surgical condition impacted select membrane properties including a transient outward current (TOC), a sustained outward current, and membrane resistance. Although the incidence of the TOC was evenly distributed across the 4 experimental groups (Table 1), the activation curves for TOC (Fig. 5B) appeared elevated for the HFD compared to the CHOW animals. Likewise, the curves for the RYGB groups were depressed. Indeed, a three-way ANOVA showed main effects for both diet (P < .03) and surgery (P < .02), but no interactions between these variables or with the level of depolarization. When examining the activation current at a single level of depolarization (−40mV), it was clear that RYGB in the HFD group tended to reduce the TOC to baseline (CHOW-SHAM) levels and to reduce the TOC in CHOW-RYGB animals below baseline

(Fig. 5C). The inactivation function for TOC exhibited similar trends for HFD to enhance and RYGB to diminish the current, but only the diet effect reached statistical significance ($P < .02$).

The effects of surgery were also evident in the sustained current (Fig. 6). There was no main effect for either surgery or diet but there was a significant interaction between surgery and applied voltage level ($P<.001$). Similar to the TOC, the sustained outward current, which was evident at the two most depolarized voltages, appeared magnified in the HFD-SHAM group and an ANOVA conducted at −45 and −40mV revealed a 3-way interaction between diet, surgery, and depolarization ($P < .05$). In addition to TOC and the sustained current, membrane resistance was significantly higher for the RYGB groups compared to the sham (ANOVA, surgery $P< .03$; diet $P > .05$, Table 1).

Despite these effects on outward current, there was no change in membrane excitability as measured by firing rate in response to injected current (Fig.7). Indeed, although there was a significant inverse correlation between TOC magnitude and maximum firing frequency ($R = −.2$; $P < .02$), this relationship only accounted for about 5% of the variance, suggesting that many other factors contribute to membrane excitability. There were, likewise, no effects of diet or surgical condition on several action potential parameters, e.g., the amplitude and half-width of the action potential or the amplitude of the afterpolarization (Table 1).

### 3.3. Rostral Solitary Nucleus

A total of 106 neurons were recorded in the rNST, defined as levels rostral to where the NST is no longer adjacent to the fourth ventricle. Neurons were recorded in a similar location regardless of group. The majority of cells were recorded from the caudal half of the rNST and in the medial half of the nucleus (Table 3, chi-squares, P's >.1). We further estimated the anteroposterior location of each cell relative to a standard atlas of the rat brain (Paxinos and Watson 1986). On average, regardless of experimental group, neurons were located just rostral to where the NST moves lateral to the IVth ventricle (mean = −12.8 ± 0.03 caudal to bregma, ANOVA, P >.1). Thus, the vast majority of rNST neurons were coincident with levels where afferent input from the glossopharyngeal and the superior laryngeal branch of the vagus nerves dominate, suggesting that most of these cells would be responsive to gustatory or tactile stimulation of the posterior oral cavity, pharynx or larynx. The remaining cells were encountered more rostrally, where neurons responsive to gustatory stimulation of the anterior tongue and palate are located (see e.g. (Hamilton and Norgren 1984; Altschuler, Bao et al. 1989; Travers and Norgren 1995)). For just over ¾ of the neurons, it was also possible to determine their locations relative to the boundaries of dense P2X2 receptor (P2X2r) fiber labeling, corresponding to the zone where primary afferents terminate (Bartel 2012). Approximately 60% of rNST neurons were in the P2X2r field whereas the others were more ventral and/or medial. Interestingly, neurons in the P2X2r field exhibited significantly larger threshold (−0.06 ± 0.15 *vs* −0.02 ± 0.03 nA) and maximal (−0.28 ± 0.07 *vs* −0.067 ± 0.01 nA) EPSC's to solitary tract stimulation (P's < .01, T-tests). However, there were no differences in location relative to the P2X2r field between groups (Table 3). Moreover, we were unable to demonstrate effects of diet or surgery on any of the parameters that we measured including incidence of a TOC, peak TOC, sustained outward

current, membrane resistance, neuron excitability to depolarizing current, or the effects of NE on responsiveness to ST stimulation (Table 3)

## 4. Discussion

Our study is one of only a few to investigate the effects of gastric bypass surgery on central neurons. We observed changes in the membrane properties of cNST neurons associated with both diet and surgery. A transient outward current, most likely an $I_A$ current, was increased with HFD. RYGB tended to reduce this current as well as a sustained outward current. In addition, the membrane resistance of neurons following RYGB was higher than sham operated animals, regardless of diet. Although the threshold for solitary tract stimulation-evoked EPSCs and the amplitude of the EPSC at threshold did not vary by condition, suprathreshold EPSCs to afferent stimulation were higher in HFD compared to chow-fed animals. In contrast to the cNST, our study did not reveal changes in the rNST as a result of either diet or surgery. This suggests that the alterations that we observed in the cNST are not ubiquitous, but selective for specific populations of neurons.

### 4.1 Survival time for HFD & RYGB

Animals on a HFD weighed significantly more than animals on a normal chow diet and RYGB significantly suppressed this differential. These effects were maintained 7 months after the diets were introduced (4.5 months after RYGB), and appeared comparable to other studies (Zheng, Shin et al. 2009). The weight differentials of our animals were also comparable to rats maintained on chow or HFD for a much shorter interval. In a study on the effects of RYGB on DMN neurons, sham or unoperated rats maintained on a HFD for 4–6 weeks weighed 33% more compared to chow fed rats (Browning, Fortna et al. 2013). In our study, animals fed the HFD weighed 21% more than chow-fed rats. Moreover, despite the vastly different time intervals between RYGB surgery and neural recording between the two studies (4.5 months *vs* 13–19 days), the weight loss following surgery was nearly identical: 33.4% *vs* 34.5% (Browning, Fortna et al. 2013). This similarity in weight loss, however, does not preclude different mechanisms controlling food intake that function at different times postoperatively.

The effects of gastric bypass surgery on metabolism and behavior involve multiple mechanisms that evolve over time (Berthoud, Shin et al. 2011; Shin, Zheng et al. 2013; Lutz and Bueter 2014). An initial phase of rapid weight loss due to non-specific surgical effects, possible “overstimulation” of the vagus from enhanced mechanical and chemical stimulation of intact vagal fibers, and possible effects of denervation from damaged vagal fibers, is followed by a second phase of slower weight loss as food intake returns to normal and a third phase of stable weight. Damage to the vagus has the potential for both short-, (0 – 40 day) (Hao, Townsend et al. 2014) and longer- term (40 – 70 day) (Bueter et al, 2010) effects on RYGB-induced weight loss. However, morphological and physiological evidence suggests considerable plasticity at the vagus–NST synapse that attenuates the effects of subdiaphragmatic vagotomy by 60 days after nerve transection (Peters, Gallaher et al. 2013).

Although the lack of a surgical effect on ST-evoked responses is consistent with a largely intact/remodeled vagus, the amplitudes of suprathreshold ST-evoked postsynaptic responses

were increased by the HFD. This alteration was somewhat unexpected in light of previous reports that responses of vagal afferents to satiety signals are decreased by a HFD (Daly, Park et al. 2011; Kentish, Li et al. 2012). Nevertheless, there is precedent for increases in ST-driven responses following other chronic conditions. For example, following chronic hypoxia, ST-evoked EPSCs at threshold were augmented, an effect attributed to both pre- and post-synaptic mechanisms, e.g increased postsynaptic glutamate sensitivity *via* increased AMPA receptor or receptor phosphorylation (Zhang, Carreno et al. 2009). Our study was not designed to parse out this kind of mechanistic detail and although a difference in the frequency or amplitude of sEPSCs might have provided some indication of the locus of the effect, we did not see any such change among experimental groups. Thus, although other mechanisms cannot be ruled out, the simplest explanation for the larger suprathreshold EPSCs is an increase in the number of synapses recruited by ST stimulation. We did not find a significant effect of diet or surgery on this measure, but our method of quantifying multiple inputs may not have been sensitive to small changes in the number of unique ST inputs, particularly those with similar thresholds. Given these limitations, it is interesting that the HFD group (particularly the HFD/Sham) had nominally more dual and triple inputs and that the HFD/RYGB group had the fewest incidences of no inputs (Table 2), a trend consistent with the significant differences in the amplitudes of the ST-evoked EPSC among these groups.

### 4.2 Intrinsic membrane properties

Of the several dependent variables that we measured, the effects of diet and surgery on a transient outward current most closely paralleled animal weight (compare Figs 2 & 5B). Animals on the chow diet had a significantly smaller TOC compared to animals on the HFD and the effects of RYGB tended to reverse this. These results are similar to those observed in DMN neurons where a HFD induced and RYGB partially reversed a shift in the $I_A$ activation curve which would have the effect of increasing the magnitude of $I_A$ current over the range of relevant membrane voltages (Browning, Fortna et al. 2013).

Although we did not specifically identify the TOC we observed as $I_A$, it exhibited the basic properties of an $I_A$ current, i.e. voltage dependency of activation, requirement of an initial hyperpolarization to deinactivate the channel, and a rapid inactivation (Cai, Li et al. 2007; Johnston, Forsythe et al. 2010; Gu and Barry 2011). Definitive identification of $I_A$ requires ion substitution to rule out the contributions of non K+ ions and a pharmacological sensitivity to 4-AP or other more specific K+ channel antagonists (Cai, Li et al. 2007; Johnston, Forsythe et al. 2010; Strube, Saliba et al. 2015;.Tsantoulas and McMahon 2014), experimental conditions incompatible with and outside the scope of our study.

We also observed changes in a sustained (composite) outward current following depolarization. RYGB suppressed this outward current at the two most depolarized levels compared to sham operated animals. These results appear to contrast with those of Browning et al (Browning, Fortna et al. 2013) who reported that RYGB increased a delayed rectifier K+ current at depolarization levels positive to 10 mV following RYGB in rats on a high-fat compared to surgical controls. Our results showed that RYGB decreased a “sustained” outward current, a current which likely included a delayed-rectifier current.

However, our results are not entirely comparable as we did not test up to 10 mV, nor specifically identify a delayed rectifier K+ channel (Johnston, Forsythe et al. 2010). In any case, the surgery-induced alterations over the voltages tested suggest underlying differences in ion channel composition that likely include multiple voltage-gated K+ channel types. Changes in K+ channel expression could also have contributed to the increased membrane resistance following RYGB, similar to that in DMN (Browning, Fortna et al. 2013). Although a HFD was reported to decrease membrane resistance in both vagal afferents at 9 weeks (Daly, Park et al. 2011) and vagal efferents at 4–6 weeks (Browning, Fortna et al. 2013), the lack of an effect in cNST could reflect the 32 week time in which our animals were on the diets.

The magnitude of a TOC can modulate neuron excitability to a depolarizing stimulus. Because the afterhyperpolarization of an action potential can deinactivate $I_A$, increases in the magnitude of $I_A$ can lead to increased interspike intervals (Amberg, Koh et al. 2003). Although we were able to demonstrate a correlation between the strength of the TOC and membrane excitability in response to a depolarizing current (Fig. 6), this correlation was weak, consistent with the lack of HFD and RYGB induced changes in excitability, despite altered TOC. Neither did we observe a decrease in excitability to a HFD as seen in dissociated nodose ganglion cells where a HFD elevated threshold (Daly, Park et al. 2011), and in the DMN where excitability was decreased, albeit only slightly (Browning, Fortna et al. 2013). It is important to note, however, that our protocols for assessing membrane excitability in response to a depolarizing current did not necessarily maximize the impact of changes in TOC on this measure (see below).

### 4.2 Role of $I_A$ in neural processing

The changes in a TOC after HFD and RYGB can potentially impact cNST processing. Bailey and colleagues showed that a hyperpolarizing prepulse, which deinactivates $I_A$, suppressed the ST-evoked response of cNST neurons that expressed this current (Bailey, Hermes et al. 2007). Thus, under a HFD where TOC is elevated, vagal afferent inputs such as satiety signals could be suppressed, particularly if they interacted with inhibitory signals from local interneurons (Chan and Sawchenko 1998; Negishi and Kawai 2011) or descending inputs (Pickel, van Bockstaele et al. 1995; Saha, Batten et al. 2000). Indeed, several studies have shown that vagally-mediated satiety-inducing manipulations, including infusions of CCK, 5-HT (Covasa, Grahn et al. 2000; Nefti, Chaumontet et al. 2009), and macronutrients (Nefti, Chaumontet et al. 2009) induce *less* Fos-like immunoreactivity in the cNST of rodents fed a HFD, suggestive of reduced neuronal excitability. However, when we tested the effects of ST stimulation we found that suprathreshold EPSCs were somewhat larger in the HFD groups. Perhaps the increased efficacy of ST stimulation that we observed is overcome or balanced by the HFD-induced decrease in vagal responsiveness to satiety signals (Daly, Park et al. 2011; Kentish, Li et al.) and increase in TOC. Thus, the increased FLI to a satiety signal in cNST neurons following RYGB (Berthoud, Shin et al. 2011) might be explained, in part, by the reduced TOC we observed post-RYGB.

Our HFD-induced change in the amplitude of the TOC would have similar consequences to the observed shift in the inactivation function for a transient K+ channel in antral circular

smooth muscle cells in diet-induced, obese-resistant rats (DIO-R) compared to obese-prone rats (Li, Maude-Griffin et al. 2013). This shift in DIO-R rats would increase the availability of K+ channels, decreasing muscle excitability and thus reduce gastric emptying compared to the obese prone rats. Similar mechanisms may exist centrally to enhance satiety following RYGB.

These changes in TOC and sustained current suggest alterations in the functional state or expression of K+ channels. Voltage-gated K+ channels, however, comprise a large and complex family and additional work is necessary to identify the precise channels (Gu and Barry 2011). For example, calcium-gated K+ channels are also implicated in response to chronic metabolic conditions: obesity appeared to suppress the expression of genes for Ca++ activated large conductance K+ currents in neurons in medial cNST (Kaneko, Yamada et al. 2009). The mechanisms through which K+ channel functional state or expression is regulated by diet or RYGB surgery are unclear. However, changes in the expression of K+ channels can be secondary to hormonal signaling (Xu, Patel et al. 2002; Khorkova and Golowasch 2007; de Lartigue, de La Serre et al. 2011) and inflammatory mediators (Tsantoulas and McMahon 2014), both of which are modulated by HFD and RYGB.

### 4.3 The role of the cNST

The cNST plays a pivotal role in feeding behavior and energy metabolism (Berthoud 2002; Grill 2010; Rinaman 2010; Rinaman 2011). It integrates afferent input from the gastrointestinal tract, is subject to a wide range of hormonal influences, and influences energy regulation and behavior through outputs to local effector systems and reciprocal connections with forebrain sites regulating metabolism and appetitive behavior. Although GI afferents terminate in virtually all cNST subdivisions, the bulk of subdiaphragmatic terminals are in the medial subdivision (Norgren and Smith 1988). Within the medial subdivisions are subpopulations of neurons that express a plethora of ligands and/or receptors for neuromodulators with orexogenic or anorexogenic properties, e.g. catecholamines, glucagon-like peptide (GLP-1), melanocortins and opioids (Larsen, Tang-Christensen et al. 1997; Berthoud 2002; Appleyard, Bailey et al. 2005; Grill 2010; Rinaman 2011; Alhadeff, Rupprecht et al. 2012; Llewellyn-Smith, Gnanamanickam et al. 2013). Some of these systems are either influenced by, or necessary to the surgical outcomes of RYGB.

For example, obesity is associated with mutations of the gene for either the ligand proopiomelanocortin (POMC) or its receptor MC4r (Andresen, Doyle et al. 2004; Hatoum, Stylopoulos et al. 2012; Zechner, Mirshahi et al. 2013), and MC4r knockout mice are refractory to weight loss following RYGB (Hatoum, Stylopoulos et al. 2012; Zechner, Mirshahi et al. 2013). Brainstem autonomic pathways are implicated in these responses as reintroduction of the MC4r into the DMN and the intermediolateral spinal cord rescued autonomic and behavioral effects of RYGB (Zechner, Mirshahi et al. 2013). In addition to the arcuate nucleus, POMC neurons are found in the medial cNST (Joseph, Pilcher et al. 1983; Appleyard, Bailey et al. 2005). It is unknown whether any of the cNST neurons with altered $I_A$ that we recorded from in the present study were POMC neurons, or whether they have direct projections to DMN. Even if this were not the case, however, it seems plausible

that the observed alterations in cNST $I_A$ could affect the relevant melanocortin circuitry indirectly, either through local connections or projections to the hypothalamus (Bailey, Hermes et al. 2007), that could then impact the brainstem *via* descending projections.

Several studies have demonstrated that the circulating levels of GLP-1 increase following RYGB, reviewed in (Lutz and Bueter 2014). Because this neuropeptide suppresses food intake (Hayes, Leichner et al. 2011), and may increase energy expenditure, (Lutz and Bueter 2014), changes in central responsiveness to this peptide would have the potential to contribute to RYGB induced weight loss. Indeed, responsiveness to GLP-1 decreased in DMN neurons in animals on a HFD and this effect reversed following RYGB (Browning, Fortna et al. 2013). Nevertheless, despite the presence of GLP-1 receptors on cNST neurons, (Llewellyn-Smith, Gnanamanickam et al.), we observed relatively little modulation by the GLP-1 analog, Exendin-4. This is also surprising in view of the location of GLP-1 receptors on nodose ganglion neurons and the increased excitability of these neurons to the application of GLP-1 agonists, mediated in part by a decrease in voltage-gated K+ currents including $I_A$ (Gaisano, Park et al. 2009). Unfortunately, we did not test for the modulation of TOC following Exendin-4 application in our study. Although the paucity of responses to Exendin are somewhat puzzling, it seems possible that this may reflect the time course of the functional effects of this agonist in NST, which have been reported to take over an hour to occur in behavioral studies (Hayes, Leichner et al. 2011). Thus, these negative results pertaining to immediate neurophysiological effects of GLP-1 do not preclude a role for NST/GLP-1 in RYGB-induced weight loss. For example, increased circulating GLP-1 could potentially influence central neurons by upregulating membrane channel expression (de Lartigue, Dimaline et al. 2007; Hayes, Leichner et al. 2011).

Both GLP-1 and catecholamine expressing neurons in the medial subdivision of the cNST are other potential subpopulations of neurons involved in modulating behavioral and autonomic responses following RYGB. Both populations of neurons respond to visceral afferents, have $I_A$, and project to both local medullary areas involved in autonomic regulation as well as forebrain sites implicated in food intake (Appleyard, Marks et al. 2007; Hisadome, Reimann et al. 2010; Rinaman 2011; Alhadeff, Rupprecht et al. 2012; Llewellyn-Smith, Gnanamanickam et al. 2013). Recent studies, however, call into question the necessity for GLP-1 for weight loss associated with RYGB (Mokadem, Zechner et al. 2013).

### 4.4 rNST

We did not observe changes in rNST neurons associated with either diet or surgery. A lack of an effect of RYGB surgery on rNST neurons is entirely consistent with observations on behavioral responsiveness to the taste stimulus, sucrose, which were made in these same rats just a brief time before our study commenced (see Fig. 1) (Mathes, Bohnenkamp et al. 2015). When Mathes and colleagues used a progressive ratio task to assess motivation to ingest small amounts of sucrose, thus limiting the impact of post-ingestive cues, there were no effects of RYGB, suggesting that the decreased preference observed in 2-bottle preference tests were more reliant on post-ingestive than gustatory factors. On the other hand, the HFD did lower the progressive ratio breakpoint, suggesting that sucrose, *per se*, was less reinforcing in rats who chronically ingested fats, a finding consistent with some

(Davis, Tracy et al. 2008; Finger, Dinan et al. 2012) though not all (la Fleur, Vanderschuren et al. 2007; Figlewicz, Jay et al. 2013) earlier studies. In any case, the present results suggest that changes in the reinforcing properties of taste stimuli brought about by a high-fat diet are not due to intrinsic changes in rNST neurons nor alterations in the efficacy of the 1st order synapse. Nevertheless, a number of prior investigations have reported considerable plasticity in gustatory brainstem responses as a function of factors related to homeostatic state, including satiety signaling (Glenn and Erickson 1976; Hajnal, Takenouchi et al. 1999), changes in blood glucose or insulin (Giza, Scott et al. 1992), and as a consequence of preference or aversion learning (Giza, Scott et al. 1992; McCaughey, Giza et al. 1997; Tokita, Shimura et al. 2007). Indeed, an investigation by Hajnal and colleagues reported leftward shifts in the parabrachial sucrose response-concentration functions in obese rats that were reversed by RYGB (Hajnal, Kovacs et al. 2010). Many possibilities exist for the locus of such effects including changes in the taste periphery (Maliphol, Garth et al.), extrinsic modulatory influences arising from the forebrain or caudal NST (Lundy and Norgren 2004; Tokita, Shimura et al. 2007; Chen, Breza et al. 2013), or intrinsic changes in rNST (or parabrachial) circuitry not explored in the current study.

## 5. Conclusion

The area of the cNST that we targeted is an important node for distributing gastrointestinal afferent signals to local reflex pathways and to the hypothalamus and other forebrain structures that influence more integrated behavioral responses. Thus, changes in membrane properties that influence excitability have the potential to have widespread influences. In particular, neurons with $I_A$ currents include medial subdivision neurons with specific input from the subdiaphragmatic vagus (Paton, Li et al. 2000), A2 catecholaminergic neurons (Appleyard, Marks et al. 2007), GLP-1 neurons (Hisadome, Reimann et al. 2010), and neurons in the medial subdivision with projections to the paraventricular nucleus (Bailey, Hermes et al. 2007). Many of these subpopulations are involved in ingestive-related functions and have widespread projections including the DMN, hypothalamus, nucleus accumbens, and other forebrain regions implicated in ingestive behavior (Berthoud 2002; Rinaman 2011; Alhadeff, Rupprecht et al. 2012; Llewellyn-Smith, Gnanamanickam et al. 2013). It is interesting that a major effect that we observed pertained to alterations in the TOC, a current with features consistent with the $I_A$ current. Thus, previous reports showing that virtually all paraventricular-projecting neurons in the medial cNST had $I_A$ compared to neurons projecting to the ventrolateral medulla (Bailey, Hermes et al. 2007) are particularly relevant to the current study because they suggest that changes in these currents may have a special impact on modifying behavior via ascending pathways.

## Acknowledgements

The authors wish to thank Jacob Harley and Devona Samuel for their hard work on data analysis. This work was supported by R01 DC000416 (SPT), R21-DC012751 to ACS, Science Foundation Ireland 12/YI/B2480 (ClR).

## References


Alhadeff AL, Rupprecht LE, et al. GLP-1 neurons in the nucleus of the solitary tract project directly to the ventral tegmental area and nucleus accumbens to control for food intake. Endocrinology. 2012; 153(2):647–658. [PubMed: 22128031]

Altschuler SM, Bao XM, et al. Viscerotopic representation of the upper alimentary tract in the rat: sensory ganglia and nuclei of the solitary and spinal trigeminal tracts. J Comp Neurol. 1989; 283(2): 248–268. [PubMed: 2738198]

Amberg GC, Koh SD, et al. A-type potassium currents in smooth muscle. Am J Physiol Cell Physiol. 2003; 284(3):C583–C595. [PubMed: 12556357]

Andresen MC, Doyle MW, et al. Differentiation of autonomic reflex control begins with cellular mechanisms at the first synapse within the nucleus tractus solitarius. Braz J Med Biol Res. 2004; 37(4):549–558. [PubMed: 15064818]

Appleyard SM, Bailey TW, et al. Proopiomelanocortin neurons in nucleus tractus solitarius are activated by visceral afferents: regulation by cholecystokinin and opioids. J Neurosci. 2005; 25(14): 3578–3585. [PubMed: 15814788]

Appleyard SM, Marks D, et al. Visceral afferents directly activate catecholamine neurons in the solitary tract nucleus. J Neurosci. 2007; 27(48):13292–13302. [PubMed: 18045923]

Attiah MA, Halpern CH, et al. Durability of Roux-en-Y gastric bypass surgery: a meta-regression study. Ann Surg. 2012; 256(2):251–254. [PubMed: 22584693]

Bailey TW, Hermes SM, et al. A-type potassium channels differentially tune afferent pathways from rat solitary tract nucleus to caudal ventrolateral medulla or paraventricular hypothalamus. J Physiol. 2007; 582(Pt 2):613–628. [PubMed: 17510187]

Banihashemi L, Rinaman L. Noradrenergic inputs to the bed nucleus of the stria terminalis and paraventricular nucleus of the hypothalamus underlie hypothalamic-pituitary-adrenal axis but not hypophagic or conditioned avoidance responses to systemic yohimbine. J Neurosci. 2006; 26(44): 11442–11453. [PubMed: 17079674]

Bartel DL. Glial responses after chorda tympani nerve injury. J Comp Neurol. 2012; 520(12):2712–2729. [PubMed: 22315167]

Berthoud HR. Multiple neural systems controlling food intake and body weight. Neurosci Biobehav Rev. 2002; 26(4):393–428. [PubMed: 12204189]

Berthoud HR, Shin AC, et al. Obesity surgery and gut-brain communication. Physiol Behav. 2011; 105(1):106–119. [PubMed: 21315095]

Bogdanske, J.; Hubbard-Van Stelle, S., et al. Laboratory Rat. Boca Raton: CRC Press; 2011.

Browning KN, Fortna SR, et al. Roux-en-Y gastric bypass reverses the effects of diet-induced obesity to inhibit the responsiveness of central vagal motoneurones. J Physiol. 2013; 591(Pt 9):2357–2372. [PubMed: 23459752]

Bueter M, Abegg K, et al. Roux-en-Y gastric bypass operation in rats. J Vis Exp. 2012; (64):e3940. [PubMed: 22710348]

Cai SQ, Li W, et al. Multiple modes of a-type potassium current regulation. Curr Pharm Des. 2007; 13(31):3178–3184. [PubMed: 18045167]

Chan RK, Sawchenko PE. Organization and transmitter specificity of medullary neurons activated by sustained hypertension: implications for understanding baroreceptor reflex circuitry. J Neurosci. 1998; 18(1):371–387. [PubMed: 9412514]

Chen Z, Breza JM, et al. Noradrenergic modulation of solitary tract-evoked activity in the rostral nucleus of the solitary tract. Society for Neuroscience Abstracts. 2013

Covasa M, Grahn J, et al. High fat maintenance diet attenuates hindbrain neuronal response to CCK. Regul Pept. 2000; 86(1–3):83–88. [PubMed: 10672906]

Daly DM, Park SJ, et al. Impaired intestinal afferent nerve satiety signalling and vagal afferent excitability in diet induced obesity in the mouse. J Physiol. 2011; 589(Pt 11):2857–2870. [PubMed: 21486762]

Davis JF, Tracy AL, et al. Exposure to elevated levels of dietary fat attenuates psychostimulant reward and mesolimbic dopamine turnover in the rat. Behav Neurosci. 2008; 122(6):1257–1263. [PubMed: 19045945]

de Lartigue G, de La Serre CB, et al. Vagal afferent neurons in high fat diet-induced obesity; intestinal microflora, gut inflammation and cholecystokinin. Physiol Behav. 2011; 105(1):100–105. [PubMed: 21376066]

de Lartigue G, Dimaline R, et al. Cocaine- and amphetamine-regulated transcript: stimulation of expression in rat vagal afferent neurons by cholecystokinin and suppression by ghrelin. J Neurosci. 2007; 27(11):2876–2882. [PubMed: 17360909]

Dockray GJ. The versatility of the vagus. Physiol Behav. 2009; 97(5):531–536. [PubMed: 19419683]

Doyle MW, Andresen MC. Reliability of monosynaptic sensory transmission in brain stem neurons in vitro. J Neurophysiol. 2001; 85(5):2213–2223. [PubMed: 11353036]

Figlewicz DP, Jay JL, et al. Moderate high fat diet increases sucrose self-administration in young rats. Appetite. 2013; 61(1):19–29. [PubMed: 23023044]

Finger BC, Dinan TG, et al. Diet-induced obesity blunts the behavioural effects of ghrelin: studies in a mouse-progressive ratio task. Psychopharmacology (Berl). 2012; 220(1):173–181. [PubMed: 21892647]

Gaisano GG, Park SJ, et al. Glucagon-like peptide-1 inhibits voltage-gated potassium currents in mouse nodose ganglion neurons. Neurogastroenterol Motil. 2009; 22(4):470–479. e111. [PubMed: 20003076]

Ganchrow D, Ganchrow JR, et al. Nucleus of the solitary tract in the C57BL/6J mouse: Subnuclear parcellation, chorda tympani nerve projections, and brainstem connections. J Comp Neurol. 2014; 522(7):1565–1596. [PubMed: 24151133]

Giza BK, Scott TR, et al. Administration of satiety factors and gustatory responsiveness in the nucleus tractus solitarius of the rat. Brain Res Bull. 1992; 28(4):637–639. [PubMed: 1617448]

Glenn JF, Erickson RP. Gastric modulation of gustatory afferent activity. Physiol Behav. 1976; 16:561–568. [PubMed: 972948]

Grill HJ. Leptin and the systems neuroscience of meal size control. Front Neuroendocrinol. 2010; 31(1):61–78. [PubMed: 19836413]

Gu C, Barry J. Function and mechanism of axonal targeting of voltage-sensitive potassium channels. Progress in Neurobiology. 2011; 94:115–132. [PubMed: 21530607]

Hajnal A, Kovacs P, et al. Gastric bypass surgery alters behavioral and neural taste functions for sweet taste in obese rats. Am J Physiol Gastrointest Liver Physiol. 2010; 299(4):G967–G979. [PubMed: 20634436]

Hajnal A, Takenouchi K, et al. Effect of intraduodenal lipid on parabrachial gustatory coding in awake rats. J Neurosci. 1999; 19(16):7182–7190. [PubMed: 10436071]

Hamilton RB, Norgren R. Central projections of gustatory nerves in the rat. J Comp Neurol. 1984; 222(4):560–577. [PubMed: 6199385]

Hao Z, Townsend RL, et al. Vagal Innervation of Intestine Contributes to Weight Loss After Roux-en-Y Gastric Bypass Surgery in Rats. Obes Surg. 2014; 24(12):2145–2151. [PubMed: 24972684]

Hatoum IJ, Stylopoulos N, et al. Melanocortin-4 receptor signaling is required for weight loss after gastric bypass surgery. J Clin Endocrinol Metab. 2012; 97(6):E1023–E1031. [PubMed: 22492873]

Hayes MR, Leichner TM, et al. Intracellular signals mediating the food intake-suppressive effects of hindbrain glucagon-like peptide-1 receptor activation. Cell Metab. 2011; 13(3):320–330. [PubMed: 21356521]

Hisadome K, Reimann F, et al. Leptin directly depolarizes preproglucagon neurons in the nucleus tractus solitarius: electrical properties of glucagon-like Peptide 1 neurons. Diabetes. 2010; 59(8): 1890–1898. [PubMed: 20522593]

Johnston J, Forsythe ID, et al. Going native: voltage-gated potassium channels controlling neuronal excitability. J Physiol. 2010; 588(Pt 17):3187–3200. [PubMed: 20519310]

Joseph SA, Pilcher WH, et al. Immunocytochemical localization of ACTH perikarya in nucleus tractus solitarius: evidence for a second opiocortin neuronal system. Neurosci Lett. 1983; 38(3):221–225. [PubMed: 6314185]

Kaneko K, Yamada T, et al. Obesity alters circadian expressions of molecular clock genes in the brainstem. Brain Res. 2009; 1263:58–68. [PubMed: 19401184]

Kentish S, Li H, et al. Diet-induced adaptation of vagal afferent function. J Physiol. 2012; 590(Pt 1): 209–221. [PubMed: 22063628]

Khorkova O, Golowasch J. Neuromodulators, not activity, control coordinated expression of ionic currents. J Neurosci. 2007; 27(32):8709–8718. [PubMed: 17687048]

la Fleur SE, Vanderschuren LJ, et al. A reciprocal interaction between food-motivated behavior and diet-induced obesity. Int J Obes (Lond). 2007; 31(8):1286–1294. [PubMed: 17325683]

Larsen PJ, Tang-Christensen M, et al. Distribution of glucagon-like peptide-1 and other preproglucagon-derived peptides in the rat hypothalamus and brainstem. Neuroscience. 1997; 77(1):257–270. [PubMed: 9044391]

Leslie DB, Dorman RB, et al. Efficacy of the Roux-en-Y gastric bypass compared to medically managed controls in meeting the American Diabetes Association composite end point goals for management of type 2 diabetes mellitus. Obes Surg. 2012; 22(3):367–374. [PubMed: 21918925]

Li S, Maude-Griffin R, et al. Gastric emptying and Ca(2+) and K(+) channels of circular smooth muscle cells in diet-induced obese prone and resistant rats. Obesity (Silver Spring). 2013; 21(2): 326–335. [PubMed: 23404843]

Llewellyn-Smith IJ, Gnanamanickam GJ, et al. Preproglucagon (PPG) neurons innervate neurochemically identified autonomic neurons in the mouse brainstem. Neuroscience. 2013; 229:130–143. [PubMed: 23069752]

Lundy, RF.; Norgren, R. Gustatory System. San Diego: Elsevier Academic Press; 2004.

Lutz TA, Bueter M. The physiology underlying Roux-en-Y gastric bypass: a status report. Am J Physiol Regul Integr Comp Physiol. 2014; 307(11):R1275–R1291. [PubMed: 25253084]

Maliphol AB, Garth DJ, et al. Diet-induced obesity reduces the responsiveness of the peripheral taste receptor cells. PLoS One. 8(11):e79403. [PubMed: 24236129]

Mathes CM, Bohnenkamp RA, et al. Gastric Bypass in Rats Does Not Decrease Appetitive Behavior Towards Sweet or Fatty Fluids Despite Blunting Preferential Intake of Sugar and Fat. Physiology & Behavior. 2015; 142:179–188. [PubMed: 25660341]

Mathes CM, Bueter M, et al. Roux-en-Y gastric bypass in rats increases sucrose taste-related motivated behavior independent of pharmacological GLP-1-receptor modulation. Am J Physiol Regul Integr Comp Physiol. 2012; 302(6):R751–R767. [PubMed: 22170618]

Mathes CM, Spector AC. Food selection and taste changes in humans after Roux-en-Y gastric bypass surgery: a direct-measures approach. Physiol Behav. 2012; 107(4):476–483. [PubMed: 22366157]

McCaughey SA, Giza BK, et al. Extinction of a conditioned taste aversion in rats: II. Neural effects in the nucleus of the solitary tract. Physiol Behav. 1997; 61(3):373–379. [PubMed: 9089755]

McDougall SJ, Peters JH, et al. Convergence of cranial visceral afferents within the solitary tract nucleus. J Neurosci. 2009; 29(41):12886–12895. [PubMed: 19828803]

Mingrone G, Panunzi S, et al. Bariatric surgery versus conventional medical therapy for type 2 diabetes. N Engl J Med. 2012; 366(17):1577–1585. [PubMed: 22449317]

Mokadem M, Zechner JF, et al. Effects of Roux-en-Y gastric bypass on energy and glucose homeostasis are preserved in two mouse models of functional glucagon-like peptide-1 deficiency. Mol Metab. 2013; 3(2):191–201. [PubMed: 24634822]

Nefti W, Chaumontet C, et al. A high-fat diet attenuates the central response to within-meal satiation signals and modifies the receptor expression of vagal afferents in mice. Am J Physiol Regul Integr Comp Physiol. 2009; 296(6):R1681–R1686. [PubMed: 19297544]

Negishi Y, Kawai Y. Geometric and functional architecture of visceral sensory microcircuitry. Brain Struct Funct. 2011; 216(1):17–30. [PubMed: 21153904]

Norgren R, Smith GP. Central distribution of subdiaphragmatic vagal branches in the rat. J Comp Neurol. 1988; 273(2):207–223. [PubMed: 3417902]

Paton JF, Li YW, et al. Properties of solitary tract neurons receiving inputs from the sub-diaphragmatic vagus nerve. Neuroscience. 2000; 95(1):141–153. [PubMed: 10619470]

Paxinos, G.; Watson, SJ. The Rat Brain in Stereotaxic Coordinates. 2nd edition. San Diego: Academic Press; 1986.

Peters JH, Gallaher ZR, et al. Withdrawal and restoration of central vagal afferents within the dorsal vagal complex following subdiaphragmatic vagotomy. J Comp Neurol. 2013; 521(15):3584–3599. [PubMed: 23749657]

Peters JH, McDougall SJ, et al. TRPV1 marks synaptic segregation of multiple convergent afferents at the rat medial solitary tract nucleus. PLoS One. 2011; 6(9):e25015. [PubMed: 21949835]

Pickel VM, van Bockstaele EJ, et al. Amygdala efferents form inhibitory-type synapses with a subpopulation of catecholaminergic neurons in the rat Nucleus tractus solitarius. J Comp Neurol. 1995; 362(4):510–523. [PubMed: 8636464]

Rinaman L. Ascending projections from the caudal visceral nucleus of the solitary tract to brain regions involved in food intake and energy expenditure. Brain Res. 2010; 1350:18–34. [PubMed: 20353764]

Rinaman L. Hindbrain noradrenergic A2 neurons: diverse roles in autonomic, endocrine, cognitive, and behavioral functions. Am J Physiol Regul Integr Comp Physiol. 2011; 300(2):R222–R235. [PubMed: 20962208]

Rinaman L, Baker EA, et al. Medullary c-Fos activation in rats after ingestion of a satiating meal. Am J Physiol. 1998; 275(1 Pt 2):R262–R268. [PubMed: 9688987]

Saha S, Batten TF, et al. A GABAergic projection from the central nucleus of the amygdala to the nucleus of the solitary tract: a combined anterograde tracing and electron microscopic immunohistochemical study. Neuroscience. 2000; 99(4):613–626. [PubMed: 10974425]

Shin AC, Zheng H, et al. Longitudinal assessment of food intake, fecal energy loss, and energy expenditure after Roux-en-Y gastric bypass surgery in high-fat-fed obese rats. Obes Surg. 2013; 23(4):531–540. [PubMed: 23269513]

Strube C, Saliba L, et al. Kv4 channels underlie A-currents with highly variable inactivation time courses but homogeneous other gating properties in the nucleus tractus solitarii. Pflugers Arch. 2015; 467(4):789–803. [PubMed: 24872163]

Suwabe T, Mistretta CM, et al. Pre- and postnatal differences in membrane, action potential, and ion channel properties of rostral nucleus of the solitary tract neurons. J Neurophysiol. 2011; 106(5): 2709–2719. [PubMed: 21865434]

Tichansky DS, Glatt AR, et al. Decrease in sweet taste in rats after gastric bypass surgery. Surg Endosc. 2011; 25(4):1176–1181. [PubMed: 20844896]

Tokita K, Shimura T, et al. Involvement of forebrain in parabrachial neuronal activation induced by aversively conditioned taste stimuli in the rat. Brain Res. 2007; 1141:188–196. [PubMed: 17276421]

Travers SP, Norgren R. Organization of orosensory responses in the nucleus of the solitary tract of rat. J Neurophysiol. 1995; 73(6):2144–2162. [PubMed: 7666129]

Tsantoulas C, McMahon SB. Opening paths to novel analgesics: the role of potassium channels in chronic pain. Trends Neurosci. 2014; 37(3):146–1s58. [PubMed: 24461875]

Xu Z, Patel KP, et al. Up-regulation of K(+) channels in diabetic rat ventricular myocytes by insulin and glutathione. Cardiovasc Res. 2002; 53(1):80–88. [PubMed: 11744015]

Zechner JF, L Mirshahi U, et al. Weight-independent effects of roux-en-Y gastric bypass on glucose homeostasis via melanocortin-4 receptors in mice and humans. Gastroenterology. 2013; 144(3): 580–590. e7. [PubMed: 23159449]

Zhang W, Carreno FR, et al. Chronic sustained hypoxia enhances both evoked EPSCs and norepinephrine inhibition of glutamatergic afferent inputs in the nucleus of the solitary tract. J Neurosci. 2009; 29(10):3093–3102. [PubMed: 19279246]

Zheng H, Shin AC, et al. Meal patterns, satiety, and food choice in a rat model of Roux-en-Y gastric bypass surgery. Am J Physiol Regul Integr Comp Physiol. 2009; 297(5):R1273–R1282. [PubMed: 19726714]

## Highlights

- A high fat diet (HFD) increases transient and sustained K+ currents in the caudal nucleus of the solitary tract
- HFD also increases the postsynaptic response to solitary tract stimulation
- RYGB surgery reverses the effects on K+ currents but not responses to afferent stimulation

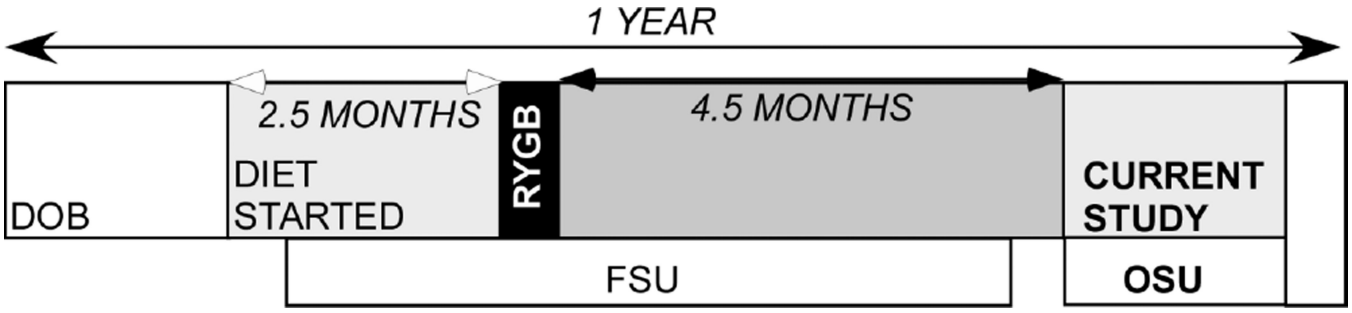


**Fig. 1.**

Time-line indicating relationships between start of diet, time of surgery and transport of the animals to Ohio State University for the patch clamp experiments.

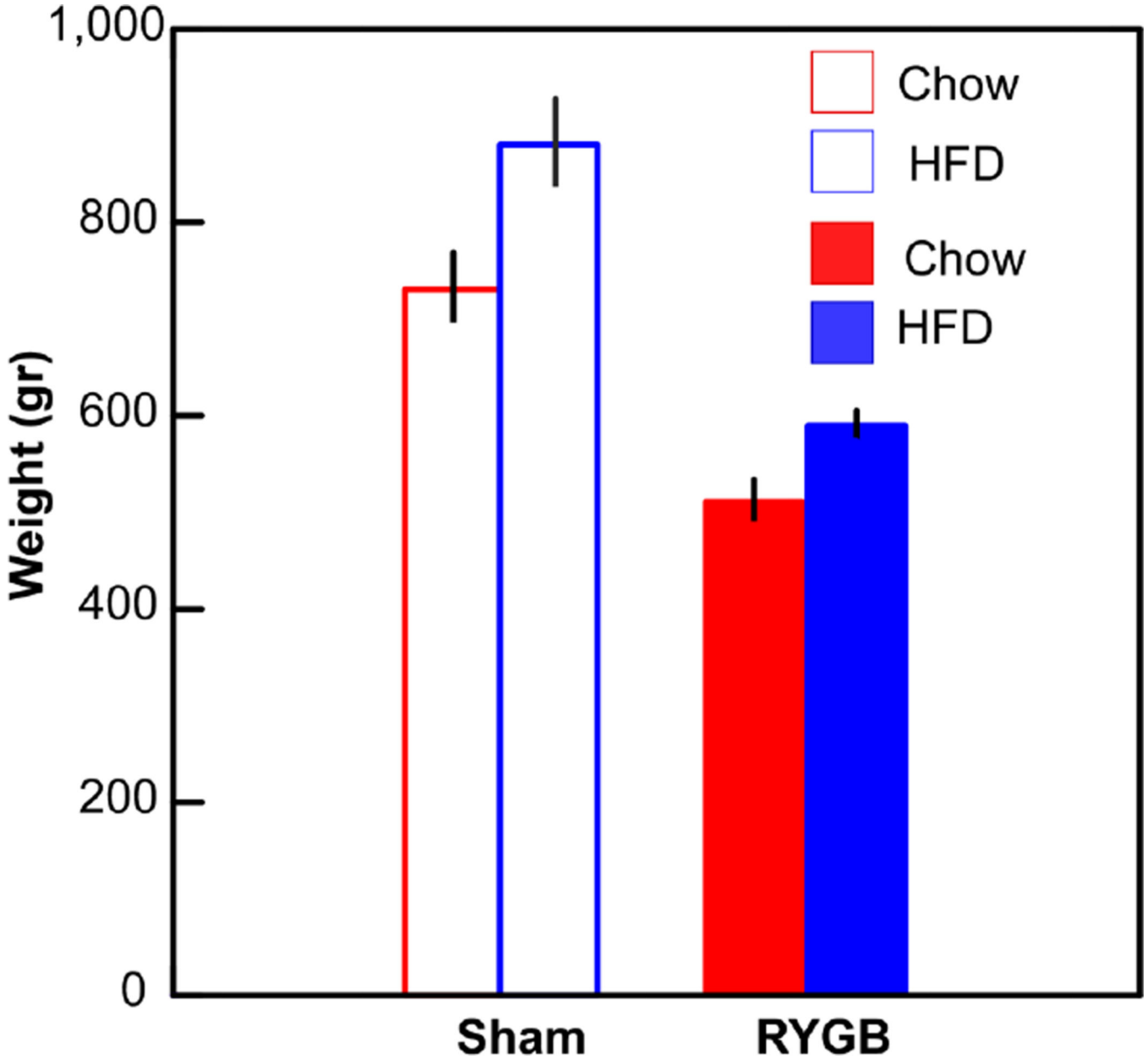


**Fig. 2.**

Weights of the animals at the time of the current study. ANOVA revealed main effects of diet ($P < .009$) and surgery ($P < .001$) but no interaction between these variables.

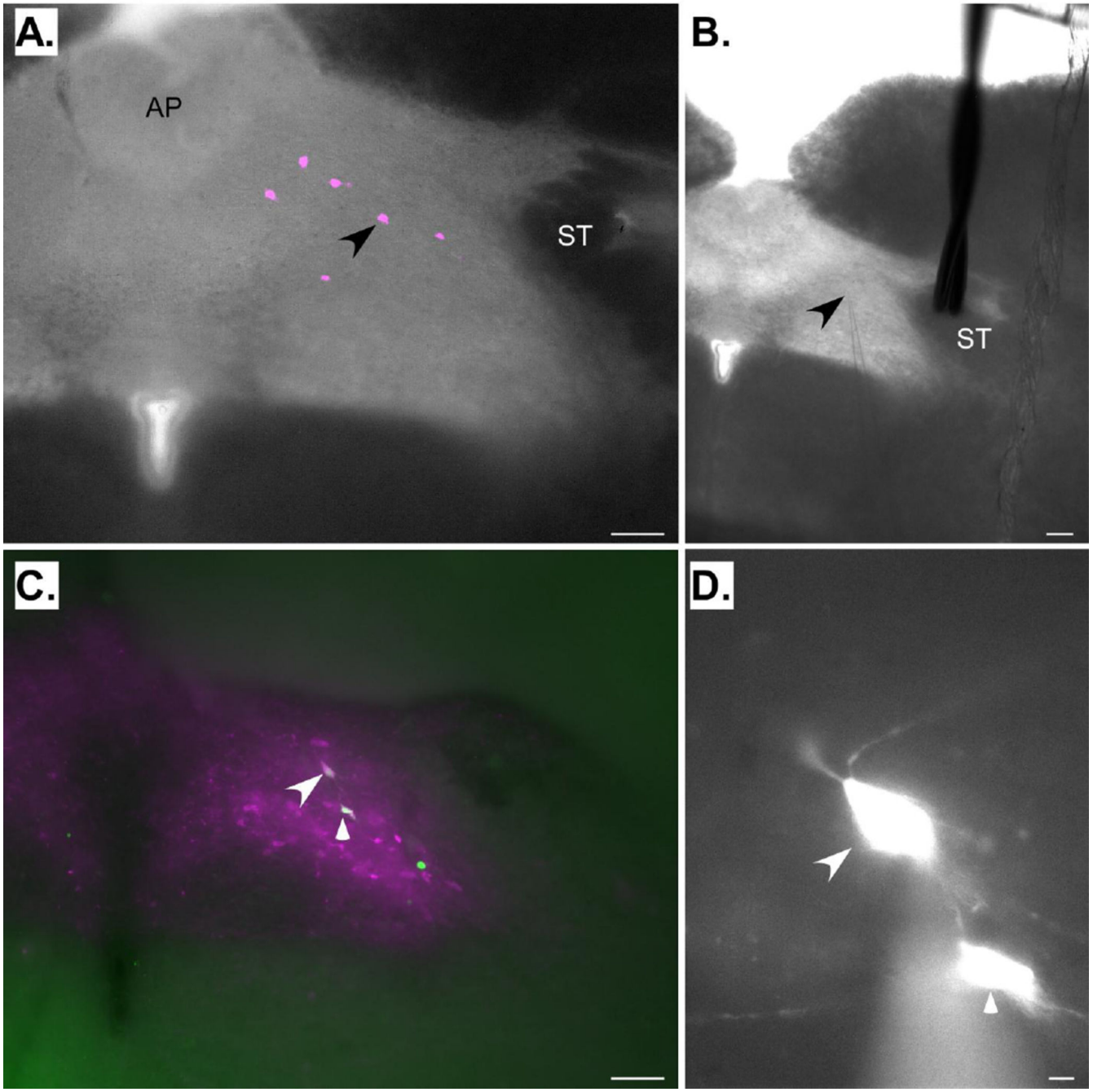


**Fig. 3.**

A and B. Photomicrographs showing a section from the cNST at the level of the area postrema (AP), the region where most cNST neurons were recorded. Panel A shows a photomicrograph of a fixed section taken after recording. Six neurons filled with Lucifer Yellow (pseudocolored magenta) are apparent. The arrowhead indicates the location of the neuron being recorded in panel B. Panel B shows a photomicrograph of the same section taken during recording. The arrow indicates the tip of the recording pipette. Note the position of the stimulating electrode on the solitary tract (ST). C. Photomicrograph of a

fixed, dopamine-beta hydroxylase-(DBH) stained cNST section taken subsequent to recording. This section was caudal to the area postrema. The arrows indicate two Lucifer Yellow-filled (pseudocolored green) neurons that are double-labeled for DBH (magenta). D. Higher-power photomicrograph of the neurons indicated in C taken during the preparation. Scale bars: 100μm in A, B, & C; 10μm in D.

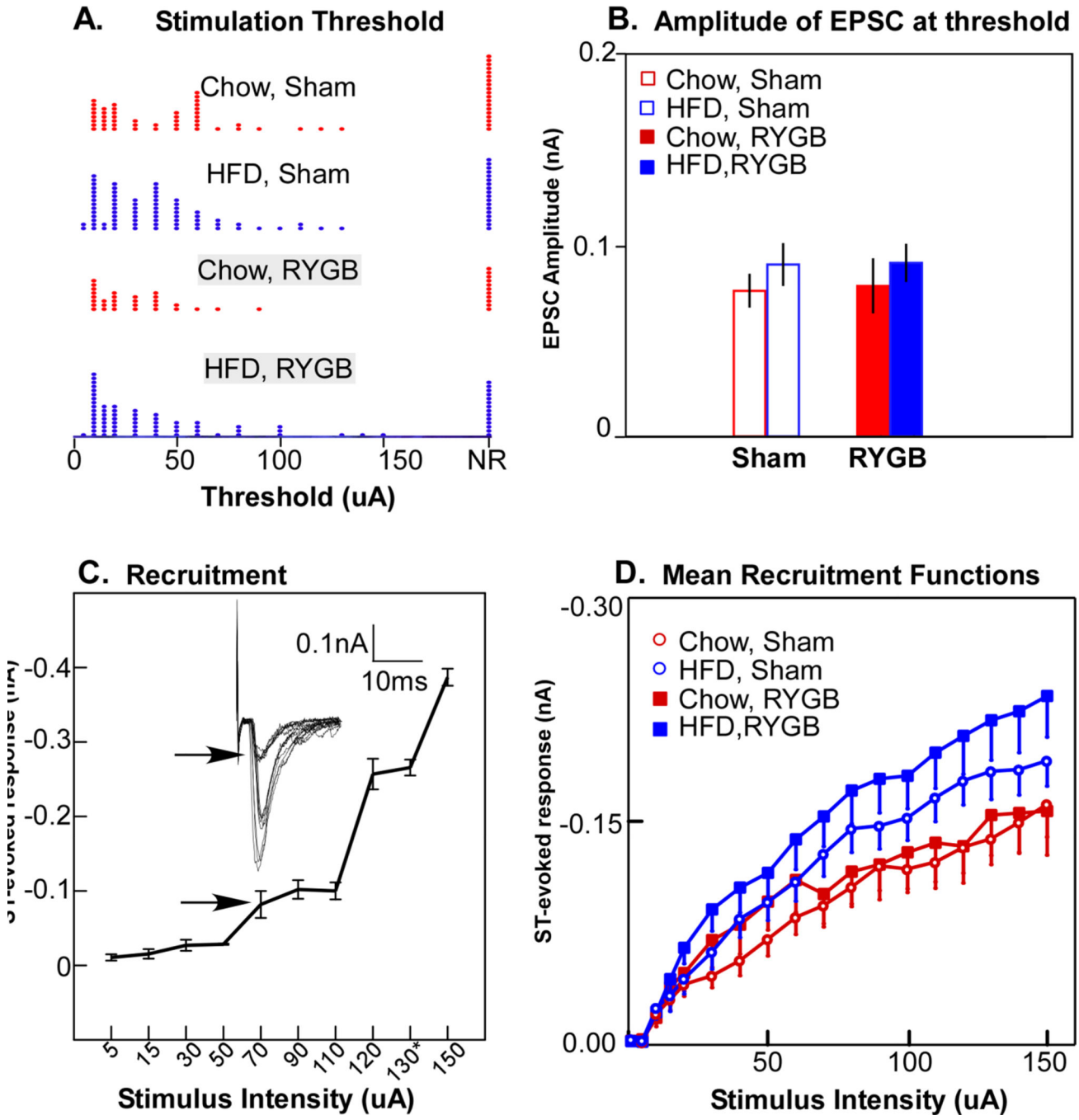


**Fig. 4.**

A. Distributions of the threshold for solitary tract (ST) stimulation necessary to elicit an excitatory postsynaptic current (EPSC) for the 4 experimental groups. NR, no reponse. B. Mean amplitude of the ESPCs at threshold; there were no significant differences across the 4 experimental groups. C. Example of recruitment of additional afferents with increases in the current amplitude of ST stimulation; 3 afferent inputs were identified for this neuron. The arrows indicate the response at threshold. D. Mean amplitudes of EPSCs at different levels of ST stimulation indicated that high fat diet (HFD) groups elicited significantly larger

EPSCs, as shown by an ANOVA with a significant main effects of diet ($P < .04$), stimulus intensity ($P < .001$) an interaction between these variables ($P < .001$), but no interaction with surgery.

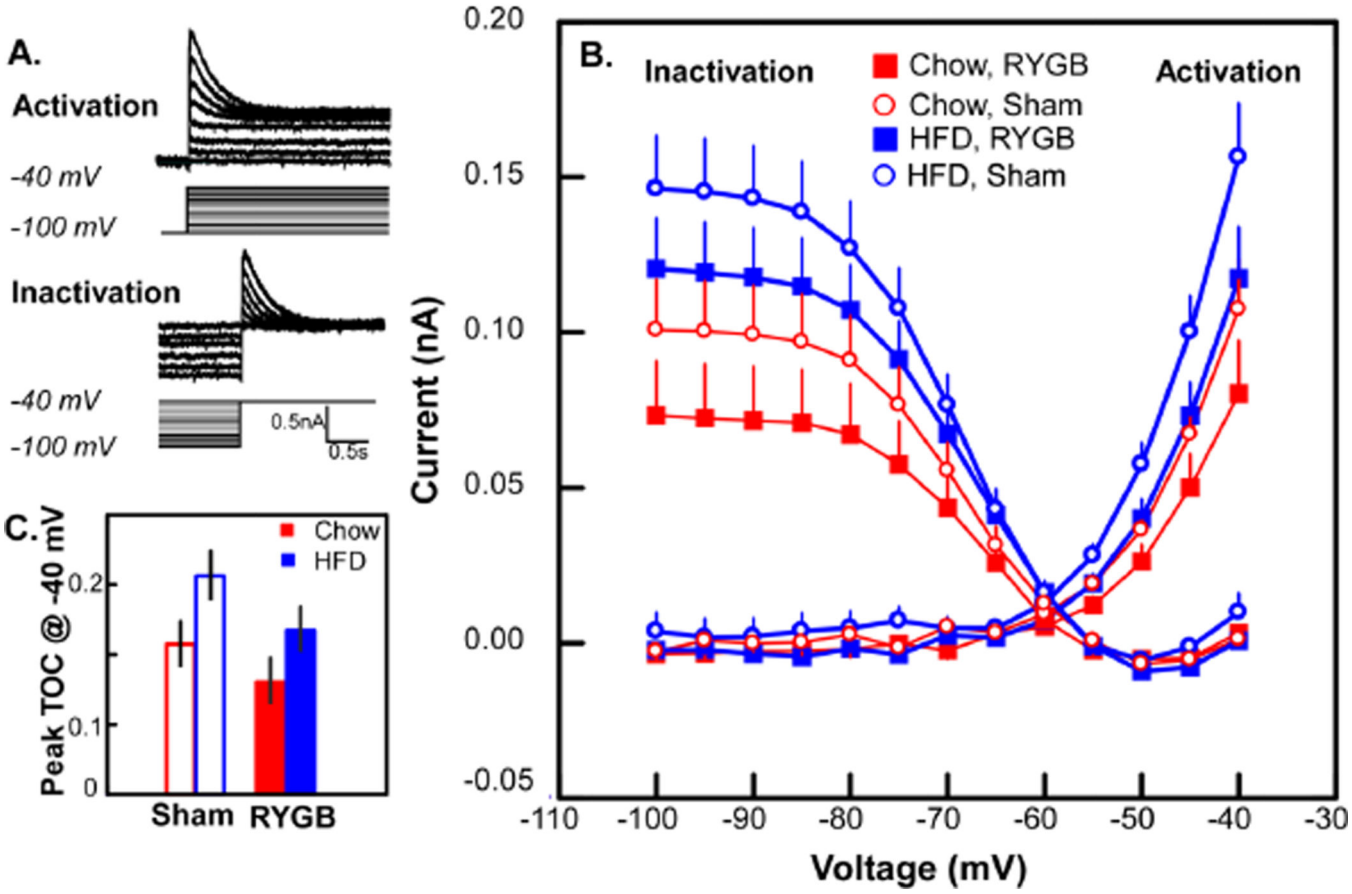


**Fig. 5.**

A. Example of the protocol for activation and inactivation for a transient outward current (TOC). For clarity, only a subset of recorded traces are shown; voltage steps for which recorded traces are not shown are designated in grey. B. Mean inactivation and activation curves for a TOC across the 4 experimental groups. ANOVA demonstrated significant main effects for both diet ($P < .03$) and surgery ($P < .02$) for the activation curve whereas only diet was significantly different for the inactivation curve ($P < .02$, see text). C. Bar graph for TOC observed at −40 mV exemplifies main effects: a high fat diet (HFD) is associated with a larger TOC and RYGB surgery suppresses the increased TOC. Note that RYGB in the HFD group reduced TOC to levels similar to sham operated chow animals.

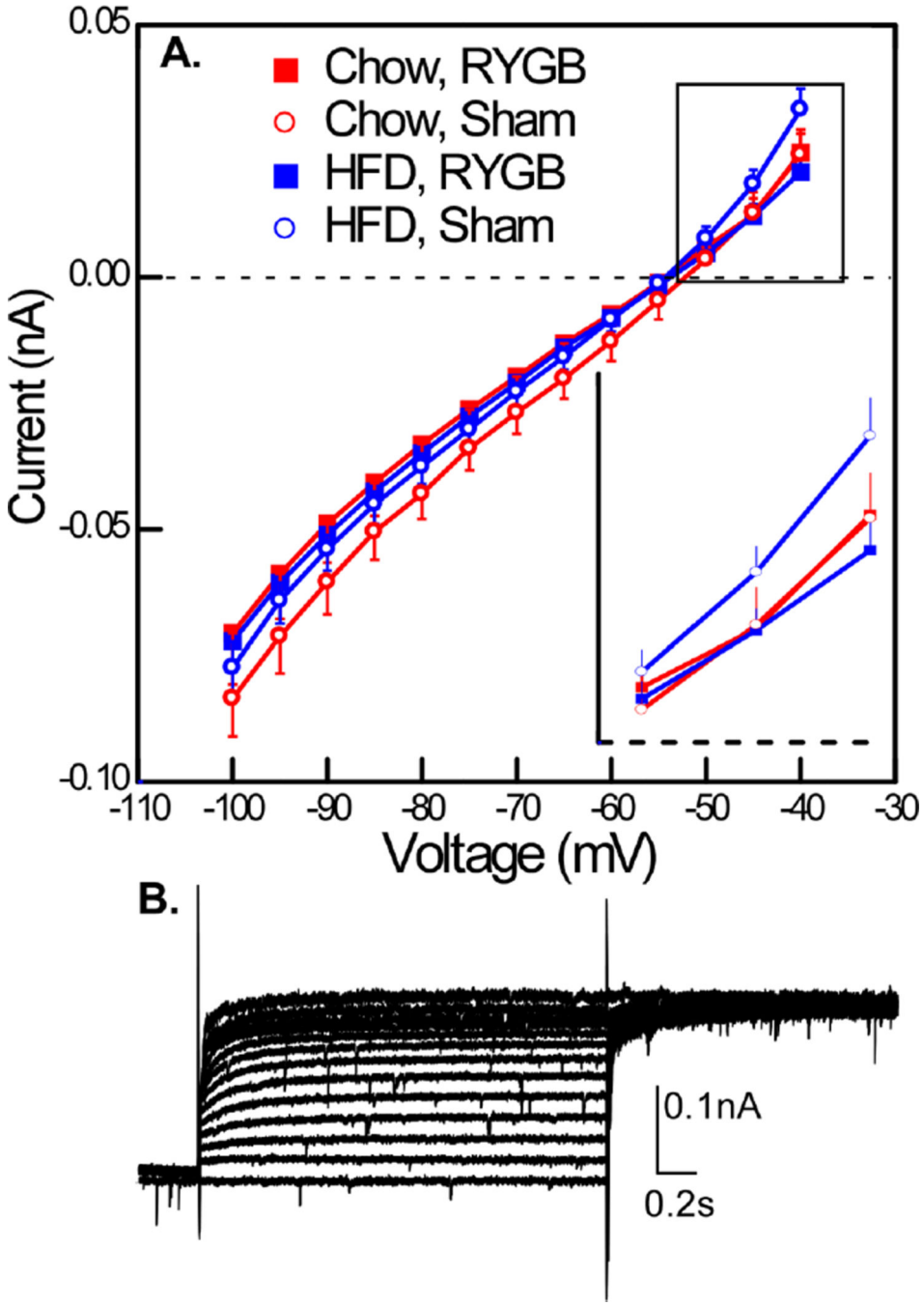


**Fig. 6.**

A. Sustained current measured at the end of the TOC activation protocol also showed effects of surgery. An ANOVA conducted over the entire curve revealed an interaction between surgery and applied voltage ($P < .001$). At the two most depolarized levels (−40 and −45mv, see inset), the outward current in the HFD sham group was magnified, and an ANOVA conducted at these levels of depolarization demonstrated a significant interaction between applied voltage, surgery and diet ($P < .05$). B. Example of sustained current in a neuron without a TOC.

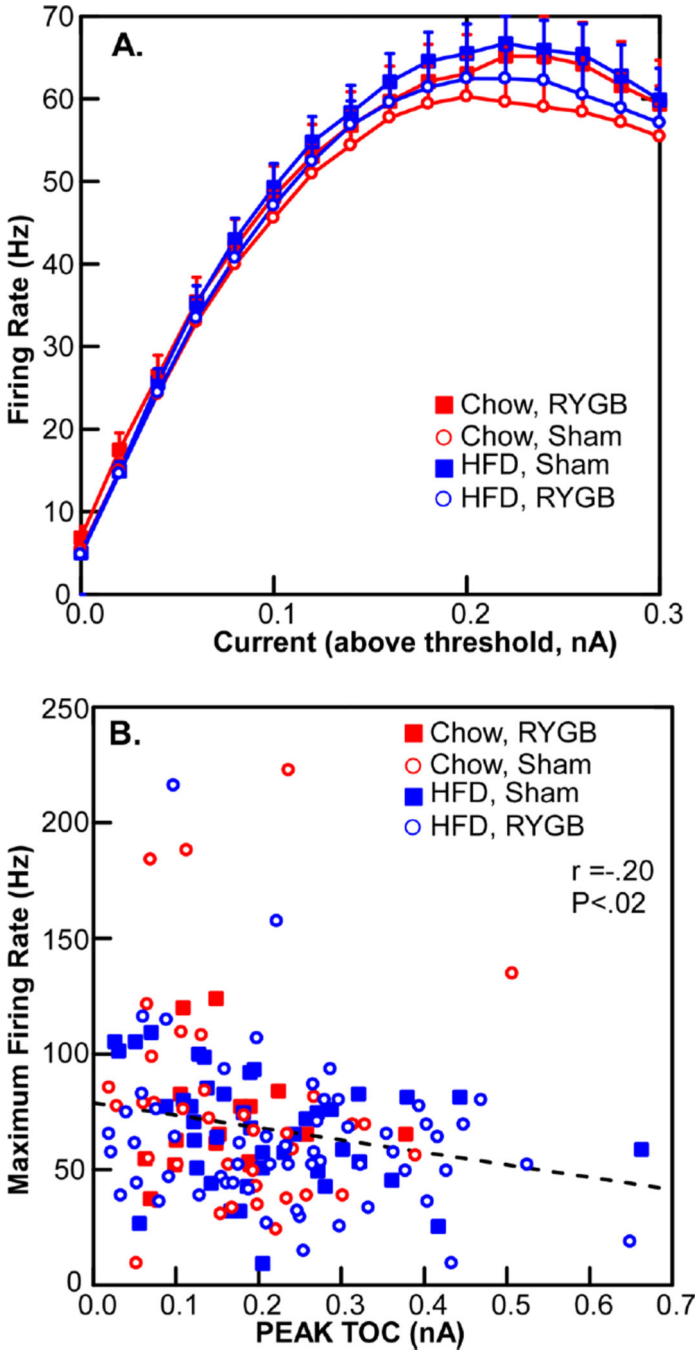


**Fig. 7.**

A. The number of action potentials in response to different levels of membrane depolarization did not change across the 4 experimental groups. B. A weak, albeit significant correlation between the magnitude of a transient outward current and maximum firing rate.

**Table 1**

cNST

| | Chow/Sham (N=7) | HFD/Sham (N=8) | Chow/RYGB (N=3) | HFD/RYGB (N=8) | Statistical Significance |
|---|---|---|---|---|---|
| **Weight (g)** | 730±36.3 | 881±45.5 | 507±23.3 | 586±15.8 | D, S |
| **Hematocrit** | 0.5±0.01 | 0.6±.04 | 0.4±0.02 | 0.4±0.02 | S |
| **Blood Glucose (mg/dL)** | 197±16.1 | 197±8.4 | 179±28.1 | 195±10.6 | NS |
| **Membrane Resistance (mΩ)** | 799±47.6 | 790± 38.6 | 945±75.2 | 874±44.3 | NS |
| **Resting Membrane Potential (mV)** | −50±9.7 | −49±8.1 | −50±8.5 | −51±8.1 | NS |
| **Action Potential Amplitude (mV)** | 95±1.7 | 93±1.2 | 95±2.0 | 96±1.3 | NS |
| **Action Potential Half Width (ms)** | 0.9±0.03 | 0.9±0.02 | 0.9±0.03 | 0.9±0.02 | NS |
| **Afterhyperpolarization Amplitude (mV)** | −37±1.6 | −37±1.1 | −32±1.6 | −37±1.2 | NS |
| **TOC +** | 62% (44) | 67% (66) | 50% (17) | 62% (52) | $\chi^2$, NS |
| **TOC −** | 38% (27) | 33% (33) | 50% (17) | 38% (32) | |
| **AP** | 84.7% (61) | 80.4% (82) | 73.2% (30) | 68.6% (59) | $\chi^2$, NS |
| **cAP** | 6.9% (5) | 15.7% (16) | 22.0% (9) | 25.6% (22) | |
| **rAP** | 8.3% 6) | 3.9% (4) | 4.9% (2) | 5.8% (5) | |

N's in the header column indicate number of animals per group.

Values indicate means ± S.E.M. or proportions expressed as percentages. The numbers of neurons appear in parentheses.

Statistical Significance indicates outcomes of ANOVA or chi-square ($\chi^2$) analyses. Significant effects: D , diet, S, surgery, NS, no significant main effects or interactions.

Abbreviations: TOC+ (transient outward current positive neurons); TOC− (transient outward current negative neurons); AP, level of the caudal solitary nucleus at the level of the area postrema; cAP, level caudal to the area postrema; rAP, level rostral to the area postrema

**Table 2**

Numbers of Inputs by Group for cNST

| Inputs | Chow/Sham | HFD/Sham | Chow/RYGB | HFD/RYGB | ANOVA |
|---|---|---|---|---|---|
| **0** | 29.7% | 20.7% | 25.6% | 19.7% | NS |
| **1** | 20.3% | 14.9% | 20.5% | 28.9% | NS |
| **2** | 29.7% | 35.6% | 33.3% | 30.3% | NS |
| **3+** | 20.3% | 28.7% | 20.5% | 21.0% | NS |

**Table 3**

rNST

| | Chow/Sham | HFD/Sham | Chow/RYGB | HFD/RYGB | Statistical Significance |
|---|---|---|---|---|---|
| **Membrane Resistance (mΩ)** | 615.4±364.6 | 473.7±261.6 | 679.7±585 | 591.9±328.3 | NS |
| **Resting Membrane Potential (mV)** | −60±7.6 | −59±10.8 | −56±10.2 | −59±10.8 | NS |
| **Action Potential Amplitude (mV)** | 62±1.6 | 58±1.8 | 63.7±3.2 | 60±2.4 | NS |
| **Action Potential Half-Width (ms)** | 1.0±0.05 | 1.1±0.04 | 0.9±0.07 | 1.0±0.05 | NS |
| **Afterhyperpolarization Amplitude (mV)** | −17±0.7 | −17±0.9 | −18±0.9 | −18.7±0.9 | NS |
| **TOC+** | 43% (9) | 44% (11) | 29% (2) | 63% (10) | $\chi^2$,NS |
| **TOC−** | 57% (12) | 56% (14) | 71% (5) | 37% (6) | $\chi^2$,NS |
| **Proportion in Caudal Half of rNST** | 86% (25) | 84% (27) | 100% (14) | 85% (22) | $\chi^2$,NS |
| **Proportion in Medial Half of rNST** | 100% (29) | 100% (32) | 100% (13) | 100% (26) | $\chi^2$,NS |
| **Proportion in P2X2r Field** | 55% (11) | 72% (21) | 50% (5) | 53% (10) | $\chi^2$,NS |